Two-loop splitting in double parton distributions.

the colour non-singlet case

May 13, 2021

M. Diehl [1] J. R. Gaunt [2] P. Plößl [1]

[1]Deutsches Elektronen-Synchrotron DESY
[2]Department of Physics and Astronomy, University of Manchester

Introduction.

What is double parton scattering?

Double parton scattering (DPS) describes two individual hard interactions in a single hadron-hadron collision:

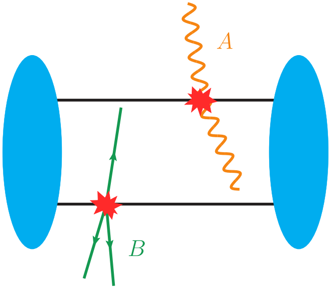

DPS is naturally associated with the situation where the final state can be separated into two subsets with individual hard scales.

⟶ DPS gives access to information about hadron structure not accessible in other processes: spatial, spin, and colour correlations between two partons!

Factorization for DPS.

Pioneering work already in the 80's:

LO factorisation formula based on a parton model picture [Politzer, 1980; Paver and Treleani, 1982; Mekhfi, 1985]

$$\sigma_{pp\to A,B} = \hat{\sigma}_{ik\to A}(x_1\bar{x}_1 s)\,\hat{\sigma}_{jl\to B}(x_2\bar{x}_2 s) \times \int \mathrm{d}^2\boldsymbol{y}\, F_{ij}(x_1, x_2, \boldsymbol{y}; Q_1^2, Q_2^2)\, F_{kl}(\bar{x}_1, \bar{x}_2, \boldsymbol{y}; Q_1^2, Q_2^2)$$

Increasing interest in DPS in the LHC era:

- First experimental data already from previous colliders at CERN and Tevatron, new measurements from LHC with more to come.
- Progress also from theory:
  - Systematic QCD description. [Blok et al., 2011; Diehl et al., 2011; Manohar and Waalewijn, 2012; Ryskin and Snigirev, 2012]
  - Factorization proof for double DY. [Diehl, Gaunt, PP, Schäfer, 2015; Diehl and Nagar, 2019]
  - Disentangling SPS and DPS. [Gaunt and Stirling, 2011; Diehl, Gaunt and Schönwald, 2017]

Factorization for DPS.

Pioneering work already in the 80's:

LO factorisation formula based on a parton model picture [Politzer, 1980; Paver and Treleani, 1982; Mekhfi, 1985]

$$\sigma_{pp\to A,B} = \hat{\sigma}_{ik\to A}(x_1\bar{x}_1 s)\,\hat{\sigma}_{jl\to B}(x_2\bar{x}_2 s) \times \int \mathrm{d}^2\boldsymbol{y}\, F_{ij}(x_1, x_2, \boldsymbol{y}; Q_1^2, Q_2^2)\, F_{kl}(\bar{x}_1, \bar{x}_2, \boldsymbol{y}; Q_1^2, Q_2^2)$$

Increasing interest in DPS in the LHC era:

- First experimental data already from previous colliders at CERN and Tevatron, new measurements from LHC with more to come.
- Progress also from theory:
  - Systematic QCD description. [Blok et al., 2011; Diehl et al., 2011; Manohar and Waalewijn, 2012; Ryskin and Snigirev, 2012]
  - Factorization proof for double DY. [Diehl, Gaunt, PP, Schäfer, 2015; Diehl and Nagar, 2019]
  - Disentangling SPS and DPS. [Gaunt and Stirling, 2011; Diehl, Gaunt and Schönwald, 2017]

Factorization for DPS.

Pioneering work already in the 80's:

LO factorisation formula based on a parton model picture [Politzer, 1980; Paver and Treleani, 1982; Mekhfi, 1985]

$$\sigma_{pp\to A,B} = \hat{\sigma}_{ik\to A}(x_1\bar{x}_1 s)\,\hat{\sigma}_{jl\to B}(x_2\bar{x}_2 s) \times \int d^2\boldsymbol{y}\, F_{ij}(x_1, x_2, \boldsymbol{y}; Q_1^2, Q_2^2)\, F_{kl}(\bar{x}_1, \bar{x}_2, \boldsymbol{y}; Q_1^2, Q_2^2)$$

Increasing interest in DPS in the LHC era:

- First experimental data already from previous colliders at CERN and Tevatron, new measurements from LHC with more to come.
- Progress also from theory:
  - Systematic QCD description.
  - Factorization proof for dDY.
  - Disentangling SPS and DPS.

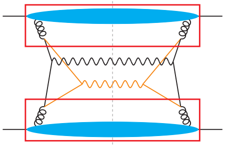

- Perturbative splitting in DPS:
  - DPS vs. SPS depends on size of transverse momenta.
  - Subtraction to solve double-counting.

Theory: DPD basics.

Definition of DPDs.

Bare position space DPDs:

$$F^{r_1 r_1' \, r_2 r_2'}_{B\text{us},a_1 a_2}(x_1, x_2, \boldsymbol{y}) = (x_1 p^+)^{-n_1} (x_2 p^+)^{-n_2} \, 2p^+ \int dy^- \frac{dz_1^-}{2\pi} \frac{dz_2^-}{2\pi} \, e^{i(x_1 z_1^- + x_2 z_2^-) p^+} \times \langle p | \, \mathcal{O}_{a_1}^{r_1 r_1'}(y, z_1) \, \mathcal{O}_{a_2}^{r_2 r_2'}(0, z_2) \, | p \rangle \big|_{y^+ = 0} \,,$$

$$\mathcal{O}_q^{ii'}(y,z) = \bar{q}_{j'}(\xi_-) \left[W^\dagger(\xi_-, v_L) \right]_{j'i'} \frac{\gamma^+}{2} \left[W(\xi_+, v_L) \right]_{ij} q_j(\xi_+) \,,$$

$$\mathcal{O}_g^{aa'}(y,z) = \left[G^{+k}(\xi_-) \right]^{b'} \left[W^\dagger(\xi_-, v_L) \right]^{b'a'} \left[W(\xi_+, v_L) \right]^{ab} \left[G^{+k}(\xi_+) \right]^{b} ,$$

with $\xi_\pm = y \pm z/2$, $z^+ = 0$, $\boldsymbol{z} = \boldsymbol{0}$.

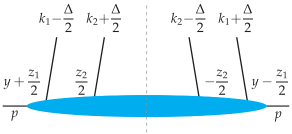

Bare momentum space DPDs:

$$F^{r_1 r_1' \, r_2 r_2'}_{B\text{us},a_1 a_2}(x_1, x_2, \boldsymbol{\Delta}) = \int d^{2-2\epsilon} \boldsymbol{y} \; e^{i \boldsymbol{y} \boldsymbol{\Delta}} \, F^{r_1 r_1' \, r_2 r_2'}_{B\text{us},a_1 a_2}(x_1, x_2, \boldsymbol{y}) \,.$$

Definition of DPDs.

Bare position space DPDs:

$$F^{r_1 r_1' \, r_2 r_2'}_{B\text{us},a_1 a_2}(x_1, x_2, \boldsymbol{y}) = (x_1 p^+)^{-n_1} (x_2 p^+)^{-n_2} \, 2p^+ \int dy^- \frac{dz_1^-}{2\pi} \frac{dz_2^-}{2\pi} \, e^{i(x_1 z_1^- + x_2 z_2^-) p^+}$$

$$\times \langle p | \, \mathcal{O}^{r_1 r_1'}_{a_1}(y, z_1) \, \mathcal{O}^{r_2 r_2'}_{a_2}(0, z_2) \, | p \rangle \big|_{y^+=0} \, ,$$

$$\mathcal{O}^{ii'}_{q}(y, z) = \bar{q}_{j'}(\xi_-) \left[W^\dagger(\xi_-, v_L) \right]_{j'i'} \frac{\gamma^+}{2} \left[W(\xi_+, v_L) \right]_{ij} q_j(\xi_+) \, ,$$

$$\mathcal{O}^{aa'}_{g}(y, z) = \left[G^{+k}(\xi_-) \right]^{b'} \left[W^\dagger(\xi_-, v_L) \right]^{b'a'} \left[W(\xi_+, v_L) \right]^{ab} \left[G^{+k}(\xi_+) \right]^{b} ,$$

with $\xi_\pm = y \pm z/2$, $z^+ = 0$, $\boldsymbol{z} = \boldsymbol{0}$.

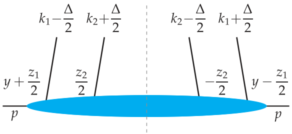

Bare momentum space DPDs:

$$F^{r_1 r_1' \, r_2 r_2'}_{B\text{us},a_1 a_2}(x_1, x_2, \boldsymbol{\Delta}) = \int d^{2-2\epsilon} \boldsymbol{y} \; e^{i\boldsymbol{y}\boldsymbol{\Delta}} \, F^{r_1 r_1' \, r_2 r_2'}_{B\text{us},a_1 a_2}(x_1, x_2, \boldsymbol{y}) \, .$$

Decomposing the colour structure of DPDs.

The colour indices in the definition of the DPDs can be coupled to an overall colour singlet in a variety of ways. [Mekhfi, 1985] In order to make this more systematic we:

- Couple the fields pairwise (r_i and r_i') to irreducible representations R_i of $SU(N)$ such that $R_1 R_2$ is a colour singlet.
- Decompose the full colour structure in terms of these combinations:

$$F^{r_1 r_1' \, r_2 r_2'}_{B\text{us},a_1 a_2}(x_1, x_2, \boldsymbol{y}) \sim \sum_{R_1, R_2} P^{r_1 r_1' \, r_2 r_2'}_{R_1 R_2} \; {}^{R_1 R_2}F_{B\text{us},a_1 a_2}(x_1, x_2, \boldsymbol{y})$$

In addition to $R_1 R_2 = 1\,1$ one finds the following colour non-singlet channels:

- $R_1 R_2 = 8\,8$ for $a_1 a_2 = q q'$.
- $R_1 R_2 = 8\,A$ and $8\,S$ for $a_1 a_2 = q g$.
- $R_1 R_2 = A\,A$, $S\,S$, $A\,S$, $S\,A$, $10\,\overline{10}$, $\overline{10}\,10$ and $27\,27$ for $a_1 a_2 = g g$.

Decomposing the colour structure of DPDs.

The colour indices in the definition of the DPDs can be coupled to an overall colour singlet in a variety of ways. [Mekhfi, 1985] In order to make this more systematic we:

- Couple the fields pairwise (r_i and r_i') to irreducible representations R_i of $SU(N)$ such that $R_1 R_2$ is a colour singlet.
- Decompose the full colour structure in terms of these combinations:

$$F^{r_1 r_1' \, r_2 r_2'}_{B\text{us},a_1 a_2}(x_1, x_2, \boldsymbol{y}) \sim \sum_{R_1,R_2} P^{r_1 r_1' \, r_2 r_2' \;\; R_1 R_2}_{R_1 R_2} F_{B\text{us},a_1 a_2}(x_1, x_2, \boldsymbol{y})$$

In addition to $R_1 R_2 = 1\,1$ one finds the following colour non-singlet channels:

- $R_1 R_2 = 8\,8$ for $a_1 a_2 = qq'$.
- $R_1 R_2 = 8\,A$ and $8\,S$ for $a_1 a_2 = qg$.
- $R_1 R_2 = A\,A$, $S\,S$, $A\,S$, $S\,A$, $10\,\overline{10}$, $\overline{10}\,10$ and $27\,27$ for $a_1 a_2 = gg$.

Rapidity divergences in colour non-singlet DPDs.

DPDs in colour non-singlet channels exhibit rapidity divergences, which cancel only when combined with the DPS soft factor [Buffing, Diehl and Kasemets, 2017]:

$$ {}^{R_1R_2}F_B(x_1,x_2,y,\zeta_p) = \lim_{\rho\to\infty} \frac{{}^{R_1R_2}F_{B\,\mathrm{us}}(x_1,x_2,y,\rho)}{\sqrt{{}^{R_1}S_B(y,2\ell_L(\rho,\zeta_p))}}\,, $$

DPS analog for TMD subtraction [Collins, 2011].

where the limit $\rho \to \infty$ corresponds to removing the rapidity regulator.

⟶ DPDs pick up a rapidity dependence, which is governed by a Collins-Soper type equation:

$$ \frac{\partial}{\partial \log \zeta_p} \log {}^{R_1R_2}F(x_1,x_2,y;\mu,\zeta_p) = {}^{R_1}J(y,\mu)/2\,, \qquad \text{with} \quad \frac{\partial}{\partial \log \mu^2}\, {}^{R}J(y;\mu) = -{}^{R}\gamma_J(\mu)\,. $$

Renormalization of UV divergences.

Renormalized position space DPDs:

$$ {}^{R_1R_2}F(x_1,x_2,y,\mu,\zeta_p) = \sum_{R_1'R_2'} {}^{R_1\overline{R}_1'}Z(\mu,x_1^2\zeta_p) \underset{1}{\otimes} {}^{R_2\overline{R}_2'}Z(\mu,x_2^2\zeta_p) \underset{2}{\otimes} {}^{R_1'R_2'}F_B(y,\mu,\zeta_p)\,. $$

with individual renormalization factors Z for each of the twist-2 operators in the definition of bare DPDs.

Double DGLAP equation for position space DPDs:

$$ \frac{\partial}{\partial \log \mu^2} {}^{R_1R_2}F_{a_1a_2}(x_1,x_2,y,\mu,\zeta_p) = \sum_{b_1,R_1'} {}^{R_1\overline{R}_1'}P_{a_1b_1}(\mu,x_1^2\zeta_p) \underset{1}{\otimes} {}^{R_1'R_2}F_{b_1a_2}(y,\mu,\zeta_p) + \sum_{b_2,R_2'} {}^{R_2\overline{R}_2'}P_{a_2b_2}(\mu,x_2^2\zeta_p) \underset{2}{\otimes} {}^{R_1R_2'}F_{a_1b_2}(y,\mu,\zeta_p)\,, $$

Perturbative splitting in DPDs.

In the limit of small distance $\boldsymbol{y}$ (and correspondingly large $\boldsymbol{\Delta}$) the leading contribution to a DPD is due to the perturbative splitting of one parton into two:

$$^{R_1R_2}F(x_1,x_2,\Delta;\mu,\zeta_p) = {}^{R_1R_2}W(\Delta;\mu,x_1x_2\zeta_p) \underset{12}{\otimes} f(\mu)\,,$$

$$^{R_1R_2}F(x_1,x_2,y;\mu,\zeta_p) = \frac{\Gamma(1-\epsilon)}{(\pi y^2)^{1-\epsilon}}\, {}^{R_1R_2}V(y;\mu,x_1x_2\zeta_p) \underset{12}{\otimes} f(\mu)\,,$$

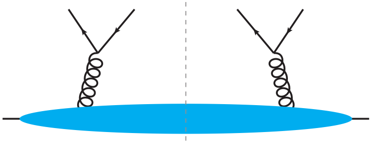

where

$$\Big[V \underset{12}{\otimes} f\Big](x_1,x_2) = \int_x^1 \frac{dz}{z^2}\, V\left(\frac{x_1}{z},\frac{x_2}{z}\right) f(z) = \frac{1}{x}\int_x^1 dz\, V(uz,\bar{u}z)\, f\left(\frac{x}{z}\right)$$

with

$$x = x_1 + x_2\,, \qquad u = \frac{x_1}{x_1+x_2}\,, \qquad \bar{u} = 1-u\,.$$

Perturbative splitting in DPDs.

In the limit of small distance $\boldsymbol{y}$ (and correspondingly large $\boldsymbol{\Delta}$) the leading contribution to a DPD is due to the perturbative splitting of one parton into two:

$$^{R_1R_2}F(x_1, x_2, \Delta; \mu, \zeta_p) = {}^{R_1R_2}W(\Delta; \mu, x_1x_2\zeta_p) \underset{12}{\otimes} f(\mu)\,,$$

$$^{R_1R_2}F(x_1, x_2, y; \mu, \zeta_p) = \frac{\Gamma(1-\epsilon)}{(\pi y^2)^{1-\epsilon}}\, {}^{R_1R_2}V(y; \mu, x_1x_2\zeta_p) \underset{12}{\otimes} f(\mu)\,,$$

formally OPE of $\mathcal{O}(y, z_1)\mathcal{O}(0, z_2)$ for $y \to 0$

where

$$\Big[V \underset{12}{\otimes} f\Big](x_1, x_2) = \int_x^1 \frac{dz}{z^2}\, V\!\left(\frac{x_1}{z}, \frac{x_2}{z}\right) f(z) = \frac{1}{x}\int_x^1 dz\, V(uz, \bar{u}z)\, f\!\left(\frac{x}{z}\right)$$

with

$$x = x_1 + x_2\,, \qquad u = \frac{x_1}{x_1 + x_2}\,, \qquad \bar{u} = 1 - u\,.$$

Calculation: Goals.

What we calculate and how we do this.

The last missing piece for NLO DPS calculations in the framework of [Diehl, Gaunt and Schönwald, 2017] are the NLO coefficients of the V splitting kernels.

⟶ Already calculated these for the colour singlet case. [Diehl, Gaunt, PP and Schäfer, 2019]

⟶ Extend this now to the colour non-singlet sector. This will also allow us to study colour correlations in DPS.

For the actual calculation we first calculate ${}^{R_1R_2}W^{(2)}_{B\,\mathrm{us}}(\Delta, \rho)$ and then extract the renormalized ${}^{R_1R_2}V^{(2)}$ by performing a RGE analysis.

We perform the calculation for two different rapidity regulators:

- Collins regulator using space-like Wilson lines. [Collins, 2011]
- δ regulator. [Echevarria, Scimemi and Vladimirov, 2016]

⟶ First application (to our knowledge) of the Collins regulator to a two loop calculation!

Goals of our calculation.

What we calculate and how we do this.

The last missing piece for NLO DPS calculations in the framework of [Diehl, Gaunt and Schönwald, 2017] are the NLO coefficients of the V splitting kernels.

⟶ Already calculated these for the colour singlet case. [Diehl, Gaunt, PP and Schäfer, 2019]

⟶ Extend this now to the colour non-singlet sector. This will also allow us to study colour correlations in DPS.

For the actual calculation we first calculate ${}^{R_1R_2}W^{(2)}_{B\,\mathrm{us}}(\Delta, \rho)$ and then extract the renormalized ${}^{R_1R_2}V^{(2)}$ by performing a RGE analysis.

We perform the calculation for two different rapidity regulators:

- Collins regulator using space-like Wilson lines. [Collins, 2011]
- δ regulator. [Echevarria, Scimemi and Vladimirov, 2016]

⟶ Obtain identical results in both schemes!

Calculation: $W^{(2)}_{B\,\mathrm{us}}$.

DESY.

From Feynman diagrams to $W^{(2)}_{B\text{us}}$.

The NLO $a_0 \to a_1 a_2$ kernel $W^{(2)}_{B\text{us},a_1 a_2,a_0}$ can be obtained by calculating the DPD for partons a_1, a_2 in parton a_0:

$$F^{(2)}_{B\text{us},a_1 a_2/a_0}(\Delta,\rho) = \sum_b \Big[W^{(2)}_{B\text{us},a_1 a_2,b}(\Delta,\rho) \underset{12}{\otimes} f^{(0)}_{B,b/a_0} + W^{(1)}_{B\text{us},a_1 a_2,b}(\Delta,\rho) \underset{12}{\otimes} f^{(1)}_{B,b/a_0} \Big] = W^{(2)}_{B\text{us},a_1 a_2,a_0}(\Delta,\rho)$$

At $\mathcal{O}(\alpha_s^2)$ we find the following splitting kernels:

- *LO* channels: $g \to gg$, $g \to q\bar{q}$, and $q \to qg$
- *NLO* channels: $g \to qg$, $q \to gg$, $q_j \to q_j q_k$, $q_j \to q_j \bar{q}_k$, $q_j \to q_k \bar{q}_k$

Note: Only *LO* channels exhibit rapidity divergences.

Calculating $W_{Bus}^{(2)}$.

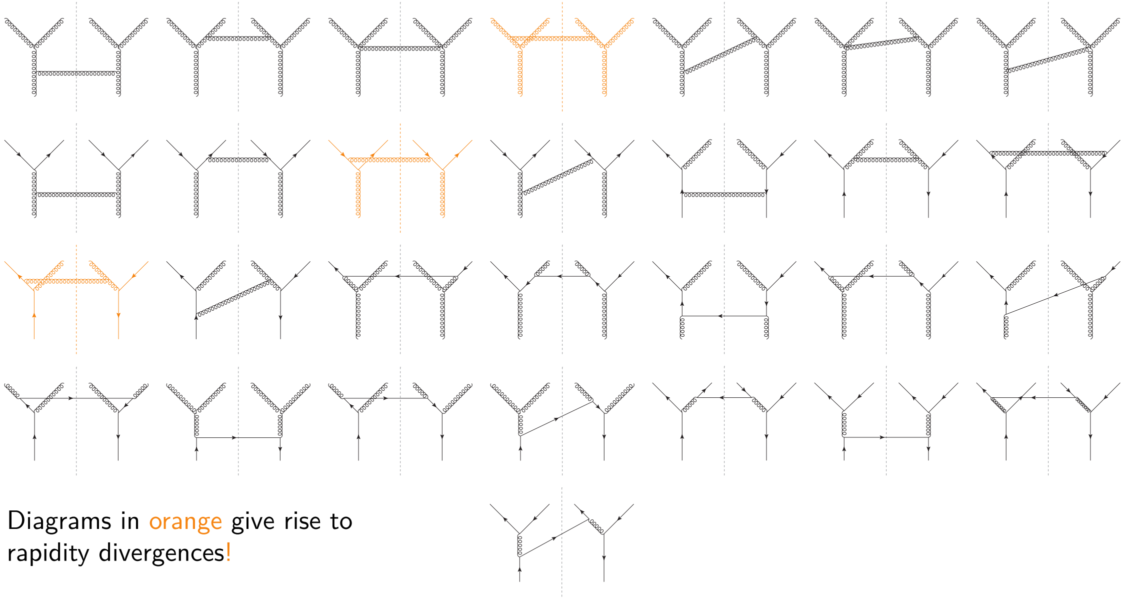

Diagrams in orange give rise to rapidity divergences!

Diagrams in orange give rise to rapidity divergences!

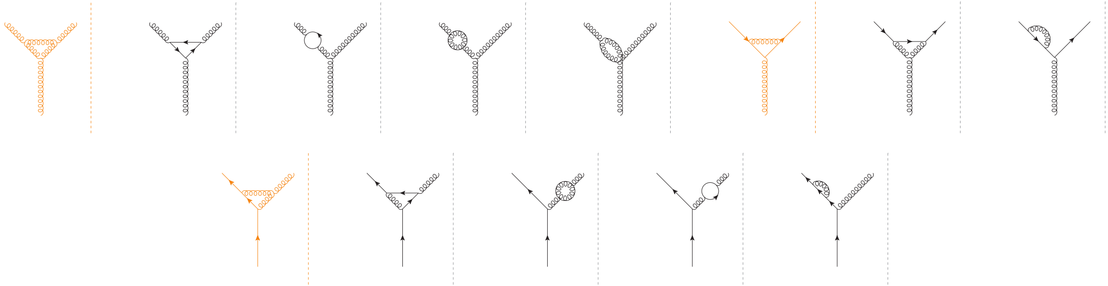

Evaluating real diagrams.

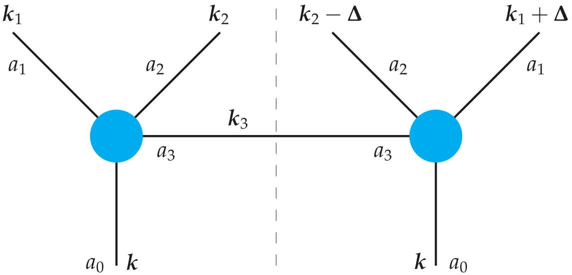

- $k_3 = k - k_1 - k_2$,
- $k_1^+ = z_1 k^+$, $k_2^+ = z_2 k^+$, $\Delta^+ = 0$
- $k_3^+ = z_3 k^+ = (1 - z_1 - z_2) k^+$

$F^{(2)}_{B\text{us}}$ and thus $W^{(2)}_{B\text{us}}$ is obtained from these diagrams by integrating over k_1^-, k_2^-, Δ^-, $\boldsymbol{k}_1$, and $\boldsymbol{k}_2$.

$\longrightarrow$ The on-shell condition for parton a_3 can be used to perform one of the minus integrations, yielding

$$k_3^- = \frac{\boldsymbol{k}_3^2}{2 z_3 k^+}$$

$\longrightarrow$ For the remaining minus integrations we use Cauchy's theorem.

How do we implement the rapidity regulators?

Wilson line propagators in the Collins and δ regulator schemes:

$$\lim_{\varepsilon\to 0}\frac{1}{v_L^- k_3^+ + v_L^+ k_3^- + i\varepsilon} + \text{c.c.} = \frac{2}{v_L^- k^+}\,\text{PV}\,\frac{z_3}{z_3^2 - \boldsymbol{k}_3^2 z_1 z_2/\rho} \qquad \text{with}\quad \rho = 2k_1^+ k_2^+\, v_L^-/|v_L^+|\,,$$

$$\frac{1}{k_3^+ + i\delta^+} + \text{c.c.} = \frac{2}{k^+}\frac{z_3}{z_3^2 + z_1 z_2/\rho} \qquad \text{with}\quad \rho = k_1^+ k_2^+/(\delta^+)^2\,.$$

In order to make the rapidity divergences which arise as z_3^{-1} poles for $\rho\to\infty$ explicit (and well defined) we perform the following distributional expansions:

$$\lim_{\rho\to\infty}\text{PV}\,\frac{z_3}{z_3^2 - \boldsymbol{k}_3^2 z_1 z_2/\rho} = \frac{1}{[z_3]_+} + \frac{1}{2}\delta(z_3)\left[\log\frac{\rho}{\boldsymbol{\Delta}^2} - \log(z_1 z_2) - \log\frac{\boldsymbol{k}_3^2}{\boldsymbol{\Delta}^2}\right],$$

$$\lim_{\rho\to\infty}\frac{z_3}{z_3^2 + z_1 z_2/\rho} = \frac{1}{[z_3]_+} + \frac{1}{2}\delta(z_3)\left[\log\rho - \log(z_1 z_2)\right].$$

Results: analytical results.

General structure of results.

Colour non-singlet kernels:

$$
{}^{R_1R_2}V^{(2)}_{a_1a_2,a_0}(z,u,y,\mu,\zeta) = {}^{R_1R_2}V^{[2,0]}_{a_1a_2,a_0}(z,u) + L\ {}^{R_1R_2}V^{[2,1]}_{a_1a_2,a_0}(z,u) + \left(L\log\frac{\mu^2}{\zeta} - \frac{L^2}{2} + c_{\overline{\text{MS}}}\right)\frac{{}^{R_1}\gamma_J^{(0)}}{2}\ {}^{R_1R_2}V^{(1)}_{a_1a_2,a_0}(z,u)
$$

where $L = \log\frac{y^2\mu^2}{b_0^2}$ and $b_0 = 2e^{-\gamma}$ and

$$
V^{[2,0]}(z,u) = V^{[2,0]}_{\text{regular}}(z,u) + \delta(1-z)\,V^{[2,0]}_{\delta}(u)\,,
$$

$$
V^{[2,1]}(z,u) = V^{[2,1]}_{\text{regular}}(z,u) + \frac{1}{[1-z]_+}\,V^{[2,1]}_{+}(u) + \delta(1-z)\,V^{[2,1]}_{\delta}(u)
$$

Results: numerical investigations.

Impact of NLO corrections on small y DPDs.

We study how including the NLO corrections effects the small y gg DPD for the following set of parameters:

- $y = 0.022\,\text{fm}$
- $\mu = \frac{b_0}{y} = 10\,\text{GeV}$
- $x_1 x_2 \zeta_p = \mu^2 = 100\,\text{GeV}^2$

For this choice of parameters only the $V^{[2,0]}$ part of the kernels contributes to the final DPD.

In order to get a feeling for the relative importance of the logarithmic $V^{[2,1]}$ and double logarithmic $V^{(1)}$ parts we vary μ and $\sqrt{x_1 x_2 \zeta_p}$ by a factor of two around their central values.

Numerics.

$\left| x_1 x_2\, {}^{RR}F_{gg} \right|$.

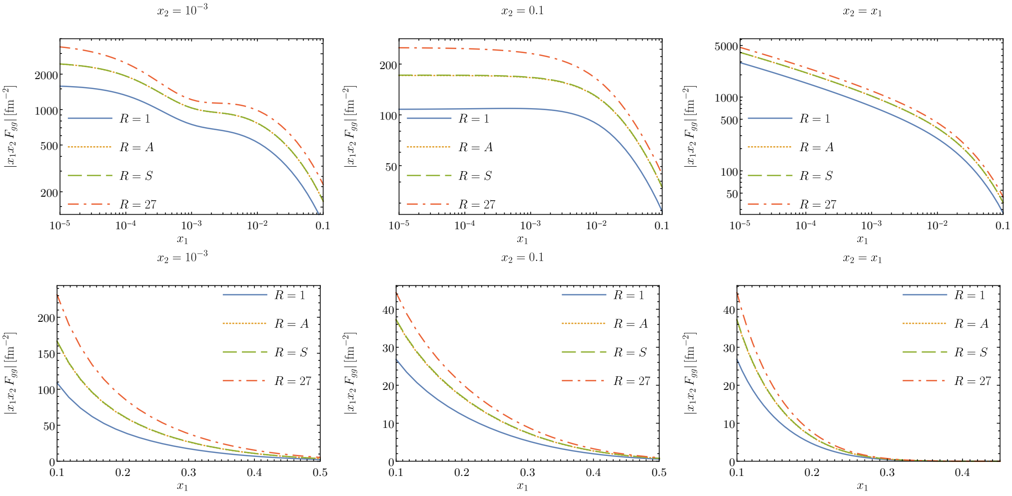

Numerics.

${}^{RR}F_{gg}^{(2)} \,/\, {}^{RR}F_{gg}^{(1)}$.

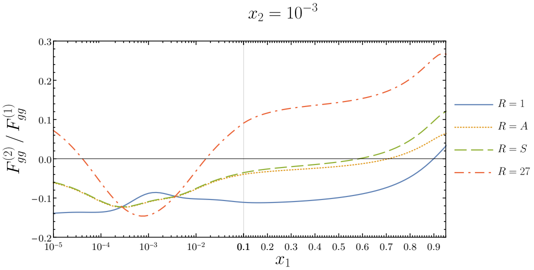

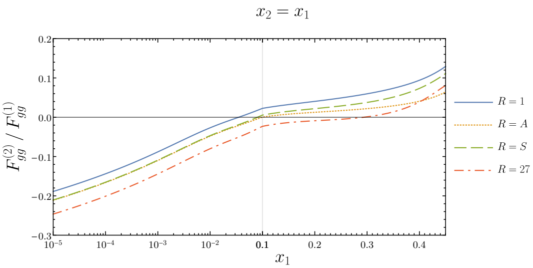

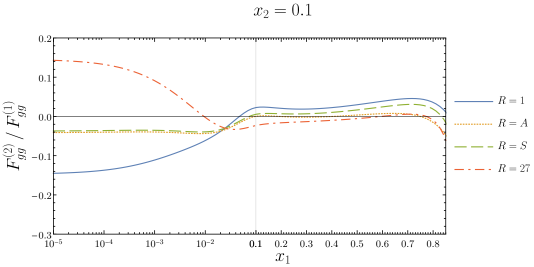

- moderate ($\mathcal{O}(10\%)$) NLO corrections.
- varied structure as a function of x_1 and x_2.
- results rather independent of PDF sets used.

Numerics.

${}^{RR}F_{gg}^{(2)} / {}^{RR}F_{gg}^{(1)}$.

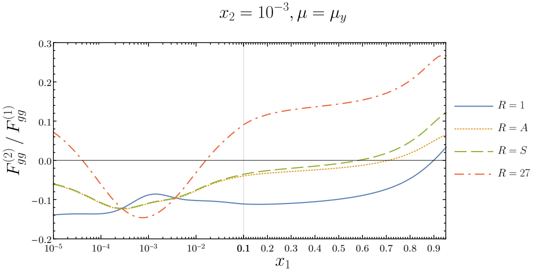

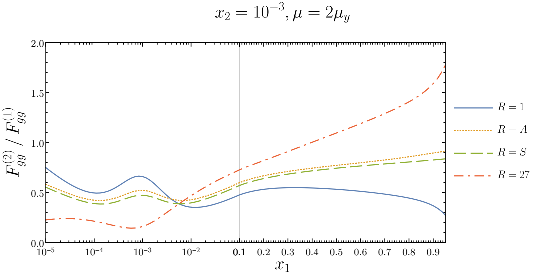

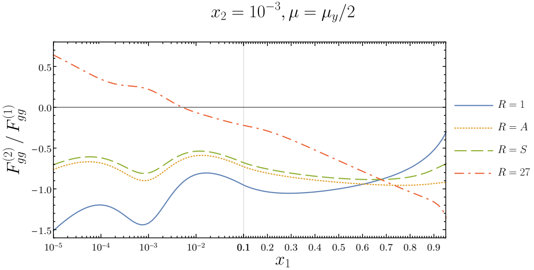

- large ($\mathcal{O}(100\%)$) NLO corrections for $\mu \neq \mu_y$.
- splitting form should be evaluated at $\mu \sim \mu_y$ to avoid large higher order corrections.

Backup.

Performing the rapidity subtraction.

A Fourier transform gives the bare unsubtracted NLO position space kernel as:

$$\frac{\Gamma(1-\epsilon)}{(\pi y^2)^{1-\epsilon}}\, {}^{R_1R_2}V^{(2)}_{B\text{us}}(y,\rho) = \int \frac{d^{2-2\epsilon}\boldsymbol{\Delta}}{(2\pi)^{2-2\epsilon}}\, e^{-i\boldsymbol{\Delta y}}\, {}^{R_1R_2}W^{(2)}_{B\text{us}}(\Delta,\rho)\,.$$

With this and the definition of the rapidity subtracted DPDs one then gets:

$${}^{R_1R_2}V^{(2)}_{B} = \lim_{\rho\to\infty}\left\{ {}^{R_1R_2}V^{(2)}_{B\text{us}}(\rho) - \frac{1}{2}\, {}^{R_1}S^{(1)}_{B}\big(2\ell_L(\rho,\zeta)\big)\, {}^{R_1R_2}V^{(1)}_{B} \right\},$$

where the involved quantities on the right-hand side generally differ in the two regulator schemes, while the left-hand side is already independent of this choice!

Performing the UV renormalization.

From the renormalization prescription for the DPDs one easily obtains that the renormalized position space splitting kernel is given by:

$$^{R_1R_2}V(y,\mu,\zeta) = {}^{R_1\overline{R}_1'}Z(\mu,\zeta) \underset{1}{\otimes} {}^{R_2\overline{R}_2'}Z(\mu,\zeta) \underset{2}{\otimes} {}^{R_1'R_2'}V_B(y,\mu,\zeta) \underset{12}{\otimes} \left({}^{11}Z\right)^{-1}(\mu)$$

The NLO position space splitting kernel $^{R_1R_2}V^{(2)}$ is then obtained by this relation in α_s to $\mathcal{O}(\alpha_s^2)$ as:

$$V^{(2)} = V_{\text{fin}}^{(2)} - \left(\hat{P}^{(0)} \underset{1}{\otimes} [V_B^{(1)}]_1 + \hat{P}^{(0)} \underset{2}{\otimes} [V_B^{(1)}]_1 - [V_B^{(1)}]_1 \underset{12}{\otimes} P^{(0)} + \frac{\beta_0}{2} [V_B^{(1)}]_1\right)$$
$$+ \left(L \log\frac{\mu^2}{\zeta} - \frac{L^2}{2} + c_{\overline{\text{MS}}}\right) \frac{\gamma_J^{(0)}}{2} V^{(1)} + L\left(\hat{P}^{(0)} \underset{1}{\otimes} V^{(1)} + \hat{P}^{(0)} \underset{2}{\otimes} V^{(1)} - V^{(1)} \underset{12}{\otimes} P^{(0)} + \frac{\beta_0}{2} V^{(1)}\right)$$

with $L = \log\frac{\mu^2 \boldsymbol{y}^2}{b_0^2}$ and $b_0 = 2e^{-\gamma}$.

Rescaling of the rapidity parameter.

The rapidity parameters ζ_p and $\zeta_{\bar{p}}$ in this work are normalised as:

$$\zeta_p \zeta_{\bar{p}} = (2p^+ \bar{p}^-)^2 = s^2 \,,$$

which differs from the convention in the TMD case

$$\zeta \bar{\zeta} = x^2 \bar{x}^2 (2p^+ \bar{p}^-)^2 = Q^4 \,,$$

where the rapidity parameters are normalized w.r.t. the extracted parton, which would be awkward in the DPD case where parton momenta often appear in convolution integrals.

$\longrightarrow$ need to rescale the rapidity parameter in renormalisation factors and evolution kernels!

$\longrightarrow$ reason: can only depend on the plus-momentum $x_i p^+$ of the parton to which they refer!

From light-cone gauge diagrams to Wilson line diagrams in Feynman gauge.

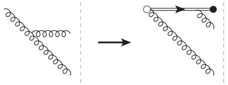

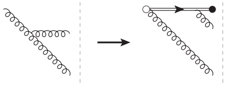

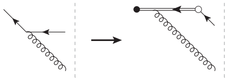

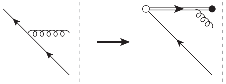

Kinematic limits of the small y DPDs.

Large $x_1 + x_2$: Plus distributions in the kernels lead to a $\log(1 - x_1 - x_2)$ enhancement in the DPDs.

- $g \to gg$, $g \to q\bar{q}$, and $q \to qg$

Small $x_1 + x_2$: For sufficiently steep PDFs the convolution integral in the small y DPD is dominated by z^{-2} terms in the kernels (in analogy to z^{-1} terms in DGLAP kernels).

- $g \to gg$, $g \to q\bar{q}$, and $q \to gg$ (in almost all colour channels)

Small x_1 or x_2: Corresponds to the small u and small $\bar{u}$ limit, with leading contributions going as u^{-1} and $\bar{u}^{-1}$ due to slow gluons.

- $g \to gg$, $q \to gg$, $g \to qg$ (u^{-1} & $\bar{u}^{-1}$),
  $q \to qg$, and $q \to qq'$ ($\bar{u}^{-1}$)

Find two sources for this behaviour in small y DPDs:

- Explicit u^{-1} and $\bar{u}^{-1}$ terms in the kernels.
- $(1 - z\bar{u})^{-1} \sim (k^+ - k_2^+)^{-1}$, $(1 - zu)^{-1} \sim (k^+ - k_1^+)^{-1}$ and similar terms.